Nanoscale Res Lett (2010) 5:1340–1343
DOI 10.1007/s11671-010-9650-x

NANO EXPRESS

Measurement of w-InN/h-BN Heterojunction Band Offsets by X-Ray Photoemission Spectroscopy

J. M. Liu · X. L. Liu · X. Q. Xu · J. Wang · C. M. Li · H. Y. Wei · S. Y. Yang · Q. S. Zhu · Y. M. Fan · X. W. Zhang · Z. G. Wang

Received: 24 March 2010 / Accepted: 17 May 2010 / Published online: 1 June 2010

Abstract X-ray photoelectron spectroscopy has been used to measure the valence band offset (VBO) of the w-InN/h-BN heterojunction. We find that it is a type-II heterojunction with the VBO being -0.30 ± 0.09 eV and the corresponding conduction band offset (CBO) being 4.99 ± 0.09 eV. The accurate determination of VBO and CBO is important for designing the w-InN/h-BN-based electronic devices.

Keywords Valence band offset · w-InN/h-BN heterojunction · X-ray photoelectron spectroscopy · Conduction band offset · Valence band offset

Introduction

Among the group-III nitrides, wurtzite InN (w-InN) is a very promising semiconductor material of application in high-frequency/high-speed/high-power heterojunction field-effect transistors (HFETs) [1–4], due to its superior electron transport properties, small effective mass, and high mobility. W-InN also has been used in field emitter because of its negative affinity (NET) [5–7]. Hexagonal boron nitride (h-BN) is a sp^2-bonded layered compound isostructural to graphite. Due to its wide band gap, it has been used in microelectronic devices. There were several reports on field emission characteristics of h-BN films [8–10]. Chinaru and his co-workers [11] designed an h-BN/GaN field emission device, which appeared lower turning on voltage compared with the conventional devices. The band structures of w-InN and h-BN are very similar to that of h-BN and GaN, so w-InN/h-BN is promising for field device. It is important to accurately determine the valence band offset (VBO) and conduction band offset (CBO) for using w-InN/h-BN-based electronic devices. Theoretical and experimental values of band structure have been extensively investigated for the w-InN and h-BN, respectively, but it is still scarce for the w-InN/h-BN heterojunction. This letter reports the valence band discontinuity at the w-InN/h-BN heterojunction interface.

Experimental

Three samples were used in our X-ray photoelectron spectroscopy (XPS) experiments. A 40-nm-thick h-BN layer was deposited by ion beam assisted deposition on Si substrate. w-InN films were deposited by metal organic chemical vapor deposition (MOCVD): a 5-nm-thick w-InN grown on a prepared h-BN layer on Si substrate and a 250-nm-thick w-InN grown on Si(111) substrate. Details of the growth conditions have been presented elsewhere [12]. The crystal qualities of w-InN were characterized using the high-resolution X-ray diffraction apparatus at Beijing Synchrotron Radiation Facility. The full width at half maximum of the X-ray diffraction rocking curve (XRC) is 0.75°. The w-InN is unintentionally n-type doped, the carrier concentration is $1 \times 10^{19}\text{cm}^{-3}$ determined by Hall performed in single field the Van der Pauw geometry at room temperature. However, the h-BN is high resistance.

J. M. Liu (✉) · X. L. Liu · X. Q. Xu · J. Wang · C. M. Li · H. Y. Wei · S. Y. Yang · Q. S. Zhu · Y. M. Fan · X. W. Zhang · Z. G. Wang
Key Laboratory of Semiconductor Materials Science, Institute of Semiconductors, Chinese Academy of Sciences, P. O. Box 912, 100083 Beijing, People's Republic of China
e-mail: liujianming@semi.ac.cn

X. L. Liu
e-mail: xlliu@semi.ac.cn

XPS measurement was performed on PHI Quantera SXM instrument with Al Kα ($h\nu = 1486.6$ eV) as the X-ray radiation source and the angle between the X-ray source and the detector is 45°. The work function and the Fermi energy level (E_F) of the instrument had been carefully calibrated. The surfaces of all the samples were exposed in the air, so existence of impurities (such as oxygen and carbon) on the surface may prevent the precise determination of the valence band maximum (VBM). In order to reduce the contamination effect, all the samples were subjected to surface clean procedure by Ar^+ bombardment with a voltage of 1 kV at a low sputtering rate of 0.5 nm/min. The total energy resolution of XPS system is about 0.5 eV, and the precision of the binding energy is within 0.03 eV after careful calibration. A low energy electron flood gun was utilized to achieve charge compensation. All XPS spectra were calibrated by the C 1-s peak at 284.8 eV from contamination to compensate the charge effect.

Results and Discussion

The VBO can be calculated according to

$$\Delta E_V = \Delta E_{\mathrm{CL}} + \left(E^{\mathrm{BN}}_{\mathrm{B1s}} - E^{\mathrm{BN}}_{\mathrm{VBM}}\right) - \left(E^{\mathrm{InN}}_{\mathrm{In3d5/2}} - E^{\mathrm{InN}}_{\mathrm{VBM}}\right), \quad (1)$$

where $\triangle E_{\mathrm{CL}} = E^{\mathrm{InN}}_{\mathrm{In3d5/2}} - E^{\mathrm{BN}}_{\mathrm{B1S}}$ is the energy difference between In $3d_{5/2}$ and B 1s CLs at the w-InN/h-BN interface. In the terms of $\left(E^{\mathrm{BN}}_{\mathrm{B1S}} - E^{\mathrm{BN}}_{\mathrm{VBM}}\right)$ and $\left(E^{\mathrm{InN}}_{\mathrm{In3d5/2}} - E^{\mathrm{InN}}_{\mathrm{VBM}}\right)$, $E^{\mathrm{BN}}_{\mathrm{In3d5/2}}$ and $E^{\mathrm{BN}}_{\mathrm{B1s}}$ are the CLs of w-InN and h-BN bulk constants of thick films, respectively, and $E^{\mathrm{BN}}_{\mathrm{VBM}}$, $E^{\mathrm{InN}}_{\mathrm{VBM}}$ means the bulk position of the valence band maximum with respect to the E_f. The CLs spectra were fitted using Voigt (mixed Lorentz–Gaussian) lineshape and Shirley background. The positions of valence band maximum (VBM) in valence band (VB) spectra are determined by linear extrapolation of leading edges of VB spectra to the base lines in order to account for the finite instrument resolution [13]. Since considerable fitted line to the original measured data has been obtained, the uncertainty of the CL positions should be lower than 0.03 eV, as evaluated by numerous fitting with different parameters. The In 3d5/2 spectra for w-InN and w-InN/h-BN samples, the B 1-s spectra for h-BN and w-InN/h-BN samples, and the valence band photoemission for both w-InN and h-BN samples are shown in Fig. 1. The parameters deduced from Fig. 1 are summarized in Table 1 for clarity. As illustrated in Fig. 1a and e, the CL lineshapes of w-InN appeared a weak asymmetry. This phenomenon had been investigated by several authors [14–17]. Stefan [18] proposed that this associated with plasmon side band. There are two types of

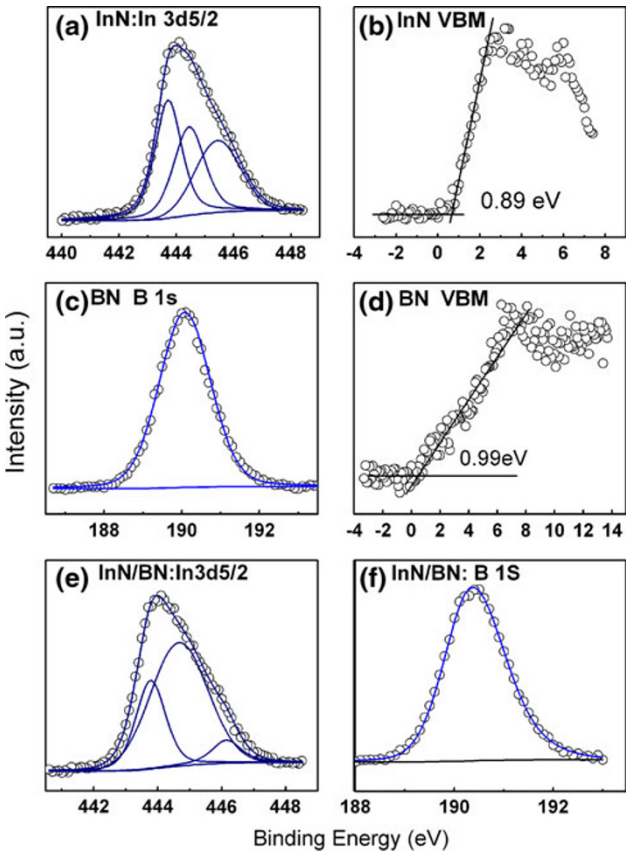

Fig. 1 CL spectra of In $3d_{5/2}$ recorded on w-InN bulk (**a**) and w-InN/h-BN (**e**) Samples, B 1-s spectra on h-BN bulk (**c**) and w-InN/h-BN heterojunction (**f**). Samples, w-InN VB spectra (**b**) and h-BN VB spectra. All peaks have been fitted to *Voigt line* shapes using Shirley background, and the VBM values are determined by linear extrapolation of the leading edge to the base line

plasmon; intrinsic plasmon and extrinsic plasmon. The intrinsic plasmon is that a strong local potential produced when an electron of CL was removed from the matrix, leaving a positive charge of photohole and then the deexcitation of the photohole by quantized excitations the conduction-electron system. However, the extrinsic plasmons are excited by the outgoing photoelectron traveling from the place of the photoexcitation process to the surface [14–17]. Energy of extrinsic plasmon is always as smooth background. Considering the couple of the surface plasmons and photoelectrons, the final-state is projected onto screened component and unscreened component [20]. We attribute the lower energy component to the "screened" final-state and the higher-energy component to the "unscreened" final-state. The latter is corresponding to a plasmon satellite at higher-binding energy. Wertheim and his co-worker [19, 20] used this model to explain screening response in narrow band metal. The energy of the surface plasmon is [17]

Table 1 Parameters (binding energy, full width at half maximum (FWHM)) of the XPS peaks and VBMs for w-InN, h-BN and w-InN/h-BN samples, the spectra as shown in Fig. 1

Samples	States	Binding energy(eV)	Bonding	FWHM(eV)
w-InN	In $3d_{5/2}$	443.71	In-N(screened)	1.09
		444.54	In-N(unscreened)	1.09
		445.45	In-O	1.09
	VBM	0.89		
h-BN	B1s	190.1	B–N	1.6
	VBM	0.99		
w-InN/h-BN	In $3d_{5/2}$	443.78	In-N(screened)	1.09
		444.67	In-N(unscreened)	2.11
		446.15	In-O	1.09
	B1s	190.37	B–N	1.3

Energy is referenced to the Fermi level (0 eV).The errors in the peak positions and VBM are ± 0.03 and 0.08 eV, respectively

$$\omega_{sp} = \left(\frac{ne^2}{(\varepsilon(\infty)+1)\varepsilon_0 m^*}\right)^{1/2}, \quad (2)$$

here n is the carrier concentration, $\varepsilon(\infty)$ and m^* are the high-frequency dielectric constant and the effective mass of the conduction electron, respectively. The ratio between surface and bulk frequencies is $\sqrt{\varepsilon(\infty)/[\varepsilon(\infty)+1]}$ with $\varepsilon(\infty) = 8.4$. The calculated result is 0.945. For the unintentionally doped n-type w-InN, the carrier concentration is much lower than that of metal. The energy of plasmon is always less than 1 eV, which is comparable with the intrinsic linewidth. The screened and unscreened peaks overlapped, resulting in an asymmetric core lineshape [19, 21]. The In $3d_{5/2}$ consists of three peaks by Voigt fit using Shirley background, the positions of peak locked at 443.71, 444.54, and 445.45 eV, as shown in Fig. 1a. The binding energy of 443.71 and 444.54 eV associated with screened final state and the unscreened final states, respectively. The binding energy of 445.45 eV belongs to In-O bond. Similarly, in the w-InN/h-BN system, the binding energy of 443.78 and 444.67 eV belong to screened and unscreen final states, respectively. According to previous reports [15], it is suggested that the energy 446.15 eV is In-O bonding in Fig. 1e.

The energy differences between the unscreened and the screened are 0.83 and 0.89 eV for the bulk and the heterojunction. It should be noted that the plasmon frequency varies with the surface electron concentration. BN 1-s peak in the bulk and heterojunction is 190.1 and 190.37 eV, respectively. The VBM lineshape and the CL positions of h-BN are very similar to the latest reports [18, 22].

Due to the peak and linewidth of higher-binding energy (unscreened final-state) depend on the excitement of bulk, surface treatment [14, 17], we choose the lower-binding energy components related to screened final-state for VBO calculation, in this letter. At room temperature, the w-InN band gap is 0.64 eV [23]. Taniguchi and his coworker have calculated the band gap of h-BN about 5.97 eV [24]. According to obtained data, the VBO is calculated to be −0.30 eV. The CBO ($\triangle E_{CBO}$) is given by the formula $\triangle E_{CBO} = \left(E_g^{BN} - E_g^{InN}\right) - E_{VBO}$. E_g^{BN} and E_g^{InN} are the band gap of h-BN and w-InN, respectively. $\triangle E_{CBO}$ is calculated to be 4.99 eV. According to these results, a type-II band alignment forms at the w-InN/h-BN heterojunction, as shown in Fig. 2.

We noted that lattice mismatch between w-InN (0001) and h-BN (0001) is 20%, so the critical thickness is estimated to be about 1 monolayer (ML). The residual stress in the film is very small. Because of the small linear pressure coefficient of InN (∼0.06 meV/Gpa) [25], the change of band gap induced by the stress can be neglected. In addition, it is well known that the nitrides are piezoelectric materials. Martin measured the piezoelectric effects of nitrides [23, 26]. According to his results, we estimate the magnitude of the field is in the order of 10^8 V/m. Due to the critical thickness is about 1 ML, the band bending caused by the piezoelectric effect is about 0.06 eV. The effect of interface states is to shift the potential within the sampled region on both sides of the interface by the same constant value. And then, any potential shift which due to band bending induced by interface states can be canceled. Considering above condition, accumulative total error is about 0.09 eV.

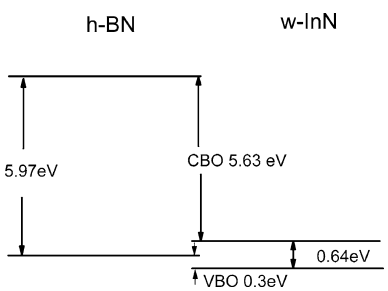

Fig. 2 Room temperature VBM and CBM line-up of the w-InN/h-BN heterojunction, showing a type-II band alignment

Conclusions

In summary, the VBO of w-InN/h-BN heterojunction has been measured by XPS to be 0.30 ± 0.09 eV, and the corresponding CBO is 4.99 ± 0.09 eV, so it belongs to a type-II band line-up. Based on the calculation, the effect of piezoelectric caused by the lattice mismatch and band bending by the surface state can be neglected. The accurate determination of the band alignment of w-InN/h-BN is important for designing the devices.

Acknowledgments The authors are grateful to Professor Huanhua Wang and Dr. Tieying Yang of the Institute of High Energy Physics, Chinese Academy of Science. This work was supported by National Science Foundation of China (No.60776015, 60976008), the Special Funds for Major State Basic Research Project (973 program) of China (No.2006 CB604907), and the 863 High Technology R&D Program of China (No.2007AA03Z402,2007AA03Z451).

References

1. S.K. O'Leary, B.E. Foutz, M.S. Shur, U.V. Bhapkar, L.F. Eastman, J Appl Phys **83**, 826 (1998)
2. B.E. Foutz, S.K. O'Leary, M.S. Shur, L.F. Eastman, J Appl Phys **85**, 7727 (1999)
3. K.T. Tsen, C. Poweleit, D.K. Ferry, H. Lu, W.J. Schaff, Appl Phys Lett **86**, 222103 (2005)
4. G. Bhuiyan, A. Hashimoto, A. Yamanoto, J Appl Phys **94**, 2779 (2003)
5. K.P. Loh, I. Sskaguchi, M.N. Gamo, S. Tagawa, T. Sugino, T. Ando, Appl Phys Lett. **74**, 28 (1999)
6. M.J. Power, M.C. Benjamin, L. Mporter, R.J. Nemanich, R.F. Davis, J.J. Cuomo, G.L. Doll, S.J. Harris, Appl Phys Lett **67**, 3129 (1995)
7. M.C. Benjamin, C. Wang, R.F. Davis, R.J. Nemanich, Appl Phys Lett **64**, 3288 (1994)
8. H.H. Busta, R.W. Pryor, J Vac Sci Technol B **16**, 1207 (1998)
9. H.H. Busta, R.W. Pryor, J Appl Phys **82**, 5148 (1997)
10. S.A. Chambers, T. Droubay, T.C. Kaspar, M. Gutocoski, J Vac Technol B **22**, 22059 (2004)
11. C. Kimura, T. Yamamoto, T. Hori, T. Sugino, J Appl Lett **79**, 4533 (2001)
12. R.Q. Zhang, P.F. Zhang, T.T. Kang, H.B. Fan, X.L. Liu, S.Y. Yang, H.Y. Wei, Q.S. Zhu, Z.G. Wang, Appl Phys Lett **91**, 162104 (2007)
13. S.W. King, C. Ronning, R.F. Davia, M.C. Benjamin, R.J. Nemanich, J Appl Phys **84**, 2086 (1998)
14. P.D. King, T.D. Veal, H. Lu, S.A. Hatfield a, W.J. Schaff, C.F. McConvill, Surf. Sci. **602**, 871 (2008)
15. P.D. King, T.D. Veal, P.H. Jefferson, C.F. Mccovine, Appl Phys Lett **90**, 1321059 (2007)
16. P.D. King, T.D. Veal, D.J. Payne, A. Bourlarge, R.G. Egdell, C.F. MoConvill, Phys. Rev. Lett. **101**, 116808 (2008)
17. V. Christou, M. Etchells, P.J. Dobson, O. Renault, G. Beamson, R.G. Egdell, J Appl Phys **88**, 5180 (2000)
18. S. Hufner, *Photoelectron spectroscopy* (Springer, Heidelberg, 1994)
19. M. Campagna, G.K. Wertheim, H.R. Shanks, F. Zumsteg, E. Bank, Phys. Rev. Lett. **34**, 738 (1975)
20. G.K. Wertheim, Chem. Phys. Lett. **65**, 377 (1979)
21. P. Widmayer, H.G. Boyen, P. Zieman, Phys Rev B **59**, 5233 (1999)
22. Y.J. Cho, C.H. Kim, H.S. Kim, J.H. Park, H.C. Choi, H.-J. Shin, G. Gao, H.S. Kang, Chem Matter **21**, 136 (2009)
23. J. Wu, W. Walukiewiewica, K.M. Yu, J.W. Ager III, E.E. Hakker, H. LU, W.J. Schaff, Y. Saito, Y. Nanishi, Appl Phys Lett **80**, 3967 (2002)
24. T. Taniguchi, H. Kanda, Nat mater. **3**, 404 (2004)
25. J. Wu, W. Walukiewiez, W. Shan, K.M. Yu, J.W. Ager III, S.X. Li, E.E. Haller, H. Lu, W.J. Schaff, Appl Phys Lett **80**, 3967 (2002)
26. G. Martin, A. Botchkatev, A. Rockett, H. Morkoc, Appl Phys Lett **68**, 2541 (1996)